Glycobiology, 2023, **33**, 11, 935–942
https://doi.org/10.1093/glycob/cwad077
Advance access publication date 4 October 2023
Communication

N-glycans show distinct spatial distribution in mouse brain

Maxence Noel[1], Richard D. Cummings[1,*], Robert G. Mealer[2,*]

[1]Department of Surgery, Beth Israel Deaconess Medical Center, Harvard Medical School, 300 Brookline Ave, Boston, MA 02215, United States, [2]Department of Psychiatry, Oregon Health & Science University, 3181 SW Sam Jackson Park Rd, Portland, OR 97239, United States
*Co-Corresponding authors: rcummin1@bidmc.harvard.edu, mealer@ohsu.edu

The development and function of the brain requires N-linked glycosylation of proteins, which is a ubiquitous modification in the secretory pathway. N-glycans have a distinct composition and undergo tight regulation in the brain, but the spatial distribution of these structures remains relatively unexplored. Here, we systematically employed carbohydrate binding lectins with differing specificities to various classes of N-glycans and appropriate controls to identify glycan expression in multiple regions of the mouse brain. Lectins binding high-mannose-type N-glycans, the most abundant class of brain N-glycans, showed diffuse staining with some punctate structures observed on high magnification. Lectins binding specific motifs of complex N-glycans, including fucose and bisecting GlcNAc, showed more partitioned labeling, including to the synapse-rich molecular layer of the cerebellum. Understanding the spatial distribution of N-glycans across the brain will aid future studies of these critical protein modifications in development and disease of the brain.

Key words: brain; glycosylation; N-glycans.

Introduction

Protein glycosylation is essential in the brain. Severe impairments of the pathway caused by Mendelian disorders of glycosylation lead to profound neurodevelopmental abnormalities (Freeze et al. 2015) and a growing body of evidence supports its role in more complex neuropsychiatric phenotypes ranging from prion disorders (Sevillano et al. 2020) to Alzheimer's disease (Suttapitugsakul et al. 2022) and schizophrenia (Mealer et al. 2022). Asparagine (N-) linked protein glycosylation has been a major focus of study in the brain (Klarić and Lauc 2022) facilitated by the ubiquitous nature of the modification, a well-defined synthetic pathway, and the facile use of tools including Peptide:N-glycosidase F (PNGase F) to release N-glycans from the protein backbone for analysis. Most work has focused on single glycan modifications in isolation or surveys on the pool of glycans present *en masse*. However, such studies often require molecular tools present only in laboratories focused on glycobiology and a niche understanding of the proper experimental controls for carbohydrate chemistry.

Lectins, carbohydrate binding proteins often isolated from plants and animals, are powerful tools in glycobiology due their relatively specific affinities to diverse types of structures (Cummings et al. 2022). However, lectins often possess a range of affinity for numerous glycans that may or may not have structural or compositional similarity, which can lead to a misinterpretation of their signal in novel contexts such as different species, tissues, and assays (Bojar et al. 2022). Lectin microarrays have been useful in examining the bulk glycan profiles across tissues (Zou et al. 2017). Pandit and colleagues presented a lectin fluorescence protocol for use in tissue sections including brain, importantly emphasizing positive and negative controls, though primary brain data was not included beyond a single representative image (Rebelo et al. 2021). Their related study investigating N-glycans in the striatum and substantia nigra nicely correlated LC-MS data and fluorescence imaging for three lectins, but did not include controls for binding, different magnification levels, or additional brain regions (Samal et al. 2020).

In this study, we combined a panel of frequently used N-glycan binding lectins with histochemical labeling of fixed mouse brain tissue, adapting lectin blotting protocols previously applied to the study of brain lysate (Williams et al. 2022). After confirming specificity of each lectin through competitive inhibition and glycosidase sensitivity, detailed imaging analysis was performed across the brain with the lectins abbreviated ConA, GNL, AAL, PHA-E, RCA, SNA, and MAL-I. Descriptions of lectin binding within the cerebellar layers are included, as well as general patterns of binding across the brain and several structures of note. These findings highlight the unique and non-uniform spatial distribution of N-glycans across the brain and provide an adaptable tool that can be utilized for the study of N-glycans in neuroscience research.

Materials and methods

All mice were maintained in standard housing conditions, provided normal chow and water ad lib, and maintained on 12-h day/light cycle. All mice were housed and maintained in accordance with the guidelines established by the Animal Care and Use Committee at Beth Israel Deaconess Medical Center under the approved protocol #02-2022. Twelve-week-old male mice on a C57BL/J6 background were used in this study unless otherwise indicated.

Histology/immunofluorescence

Mice at 12 weeks of age were euthanized with CO_2 gas in accordance with AVMA guidelines and trans-cardially perfused with ice-cold PBS containing heparin at 10,000 units/L (Sigma #3149) for 2 min at 6 mL/min, followed by ice-cold 4% PFA in 0.1 M PBS, pH 7.4 for 5 min at 5 mL/min. Whole brains were then removed from the skull and post-fixed in 4% PFA overnight and transferred to PBS until

Received: June 15, 2023. **Revised:** September 24, 2023. **Accepted:** September 9, 2023

processing. Fixed brain was paraffin embedded and cut in 3 μm coronal sections with a microtome at the BIDMC Pathology Core Facility. Slides were then deparaffinized using a standard xylene/ethanol gradient protocol and placed in antigen retrieval solution (0.1 M citric acid and 0.1 M sodium citrate, pH = 6), incubated in pressure cooker at boiling temperature for 3 min, and stored at 4 °C in TBS. Tissue sections were circled by hydrophobic PAP PEN and slides were treated with 1X denaturing buffer containing 0.5% SDS, 40 mM DTT (NEB: P1704S) for 5 min at 95 °C. Sections were washed with TBS (Trizma 20 mM, NaCl 100 mM, $CaCl_2$ 1 mM, $MgCl_2$ 1 mM, pH 7.2) 3 times followed by 3 washes with TBS-tween 0.05% (TBS-T). Sections were blocked with 3% BSA in TBS for 1 h at room temperature (RT). Tissues were washed again three times with TBS and incubated with 25 μg/mL of lectins (Vector Labs: ConA FL-1001, GNL B-1245, AAL FL-1391, PHA-E FL-1121, RCA-I B-1085, SNA FL-1301, MAL-I FL-1311) in TBS-T for 1 h at RT in darkness with gentle shaking. For control glycosidase experiments, slides were pretreated with 2,500 U of PNGase F (NEB: P0704) in a final volume of 80 μL at 37 °C for 1 h prior to incubation with lectins. For control carbohydrate/haptenic sugar blocking experiments, lectins were incubated for 30 min with the indicated sugar before incubation on the slide for 1 h at RT. After the incubation with lectins, sections were washed with TBS-T 3 times. Most lectins described above were directly conjugated to FITC – however, for biotinylated RCA-I and GNL, streptavidin-488 (Invitrogen, S11223) was used as secondary antibody at 10 μg/mL and incubated in TBS-T for 1 h at 25 °C prior to imaging. Sections were washed 2 times with TBS-T, one time with TBS and counterstained with Hoechst 33,342 diluted at 1/1,000 in TBS for 10 min at RT in darkness. Sections were then washed 3 times with TBS, incubated with 0.1% Sudan Black B (Sigma, 199664) in 70% ethanol for 5 min to reduce autofluorescence coming from lipofuscin, washed again 2 times with TBS and mounted with a glass coverslip using Prolong Gold Antifade Mountant (ThermoFisher, P36930). After slides cured overnight, image acquisition was performed on Zeiss LSM 880 Upright Confocal System at the BIDMC Confocal Microscopy Core for high magnification and a VS120 Slidescanner from Olympus for low magnification. Images analysis was then performed using ImageJ (v1.53t) or QuPath (v0.3.2) software.

Results

To ensure precise interpretation of lectin staining to coronal mouse brain sections, we generated a standardized protocol which was then adapted for each lectin on sections in which glycolipids were removed through the process of tissue processing. After observing binding to brain sections, specificity was confirmed by both sensitivity to glycosidase treatment and inhibition with competing carbohydrates (haptens) based on previous characterizations and the recommendations by the commercial suppliers (Fig. 1A). Because lectins can bind a similar epitope on different glycoconjugates, such as glycoproteins with differing linkages and/or protein attachments, these controls provide additional information when interpretating the results. In addition, fluorescently labeled and biotinylated lectins, which are commercially available, were confirmed for their specificity by glycan microarray analyses using resources at the National Center for Functional Glycomics (NCFG). The lectins used and references for their specificities include Concanavalin A (ConA) (Kornfeld and Ferris 1975; Baenziger and Fiete 1979), *Galanthus nivalis* lectin (GNL) (Kaku and Goldstein 1989; Wright and Hester 1996), *Aleuria aurantia* lectin (AAL) (Yamashita et al. 1985), *Phaseolus vulgaris* erythroagglutinin-E (PHA-E) (Cummings and Kornfeld 1982), *Ricinus communis* agglutinin-I (RCA) (Baenziger and Fiete 1979), *Sambucus nigra* agglutinin (SNA) (Shibuya et al. 1987), and *Maackia amurensis* lectin (MAL-I) (Wang and Cummings 1988; Geisler and Jarvis 2011). Using cerebellar tissue, the binding of the commonly used lectin ConA to the mannose core of most N-glycans was confirmed by signal loss following treatment with Peptide:N-glycosidase F (PNGase F) that removes all types of N-glycans, and by competitive inhibition of lectin binding with 200 mM glucose and 200 mM mannose (Fig. 1B).

High magnification images at the Purkinje cell layer junction of the cerebellum highlight several unique characteristics of N-glycan lectin binding patterns, including the presence of punctate structures, varying degrees of staining across anatomical layers, and binding to luminal structures (Fig. 2). We next focused on binding patterns across the brain, utilizing three coronal planes to survey numerous macroscopic structures including cerebellum, brain stem, corpus callosum, hippocampus, thalamus, hypothalamus, cortex, and olfactory bulb (Fig. 3A and B, Supplementary Fig. 1). Differential binding patterns were observed for each lectin, as detailed below, and summarized in Table 1.

The lectin ConA, which binds mannose within high mannose, hybrid, and biantennary complex-type N-glycans, showed diffuse staining across nearly every region of the brain (Supplementary Fig. 2). Specificity of the signal was confirmed by PNGase F treatment and inhibition with 200 mM mannose and 200 mM glucose. In the cerebellum, ConA binding appeared highest in the molecular layer (ML), with less in the granular layer (GL), and the least in the arbor vitae (AV). This diffuse pattern was present across the more rostral brain structures, with a decreased signal present in white matter tracts including the corpus callosum. Several punctate structures were noted in and around the cell bodies of the Purkinje cell layer.

GNL, which binds terminal α-linked mannose commonly found on high mannose and hybrid-type N-glycans, and notably does not bind to complex-type N-glycans, also showed diffuse distribution across the brain with increased signal observed in the glomerular layer of the olfactory bulb (Supplementary Fig. 3). Specificity of the signal was confirmed by PNGase F treatment and inhibition with 200 mM mannose and 200 mM glucose, which removed the bulk of the signal. The minor residual background could result from non-specific signal, incomplete on-slide digestion as this lectin binds the most abundant class of N-glycans in the brain, or binding to other glycoconjugates such as terminal O-linked mannose on cadherins (Larsen et al. 2017). The latter seems unlikely, however, as nearly all GNL binding to brain lysate on lectin blots is removed by both PNGase F and Endo H, a glycosidase specific for high mannose and hybrid-type N-glycans, and we did not previously identify any structures consistent with terminal O-linked mannose via MALDI-MS (Williams et al. 2022). In the cerebellum, near equal intensity of GNL binding was observed in the ML and GL, with reduced intensity in the AV. Similar to ConA, high magnification showed punctate structures binding GNL in the Purkinje cell layer.

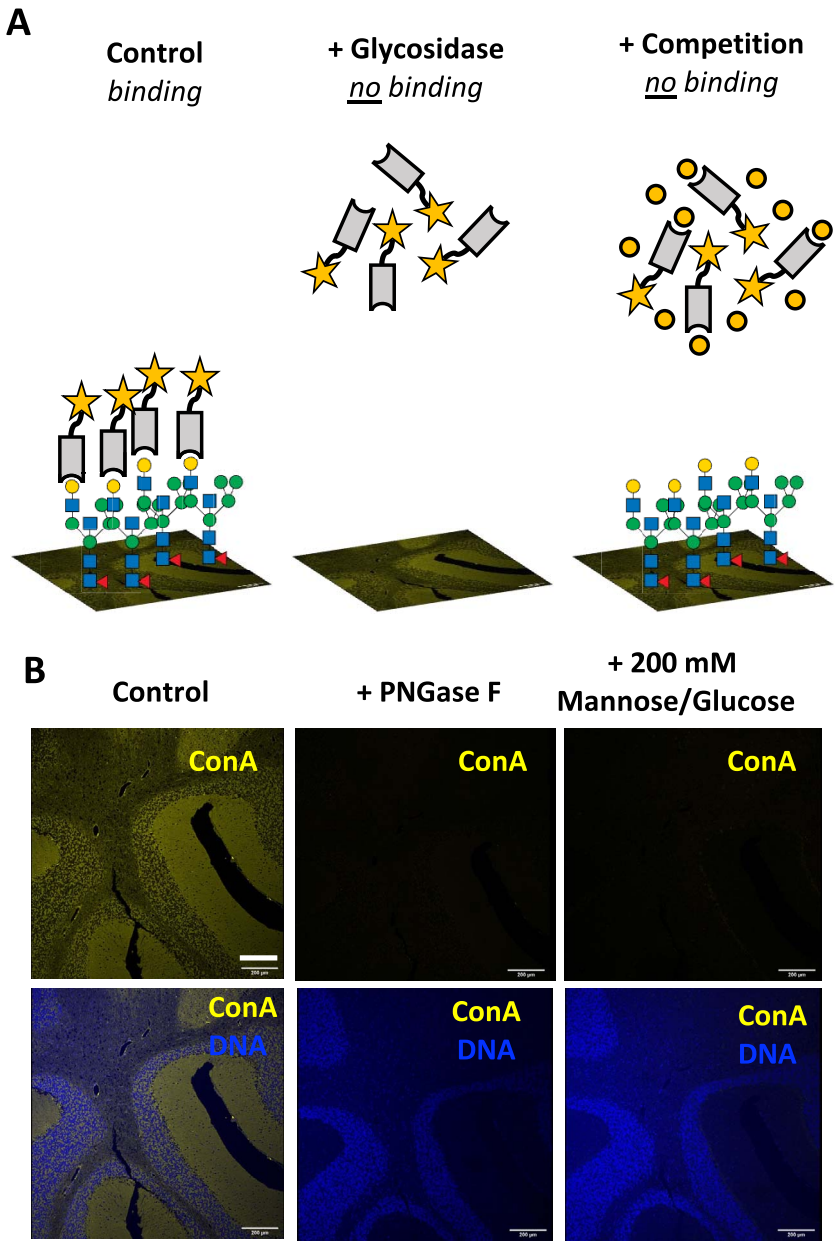

Fig. 1. Optimized lectin fluorescence in brain slices. A) Schematic highlighting controls for determining specific binding of lectins to brain slices. The binding of lectins with a reporter such as a fluorescent tag (star) reveals the spatial distribution of glycan classes on a tissue slide. Specific binding of the lectin to the glycan structures is confirmed by determining its sensitivity to appropriate glycosidases as well as through inhibition under saturating concentrations of a competitive carbohydrate. B) The specificity of ConA binding to its substrate on the layers of the cerebellum is confirmed via removal of the N-glycans by incubation with PNGase F and inhibition of the lectin binding by saturating conditions of mannose and glucose (200 mM each). Scale bar = 200 μm. Panels from B are presented in supplemental material with additional context for ConA and other lectins.

AAL, which binds nearly all linkages of fucose to N-glycans, showed broad staining but considerable layering in certain areas (Supplementary Fig. 4). Specificity of the signal was confirmed by PNGase F treatment and inhibition with 200 mM L-fucose. As AAL fluorescence is entirely removed by PNGase F, in agreement with our previously published blotting results with brain lysate (Williams et al. 2022), we conclude that the bulk AAL signal in the brain is present on N-glycans with minimal contribution from other potential glycoconjugates such as O-linked glycans. In the cerebellum, AAL signal was dramatically enriched in the ML compared to both the GL and AV. Though some punctate structures were noted on high magnification, these appeared more diffusely spread across the ML.

PHA-E, which has affinity for bisected N-glycans containing a β-1,4 linked GlcNAc to the core mannose, showed a pattern similar to AAL (Supplementary Fig. 5). Specificity of the signal was confirmed by PNGase F treatment and inhibition with 200 mM GalNAc and lactose. PHA-E binding highlights the complexity and limitations of single controls such as competitive hapten sugars, as the only known inhibitor for PHA-E is GalNAc, despite this monosaccharide not being present in the major glycan structures to which PHA-E is reported to bind (Cummings et al. 2022). Thus, the

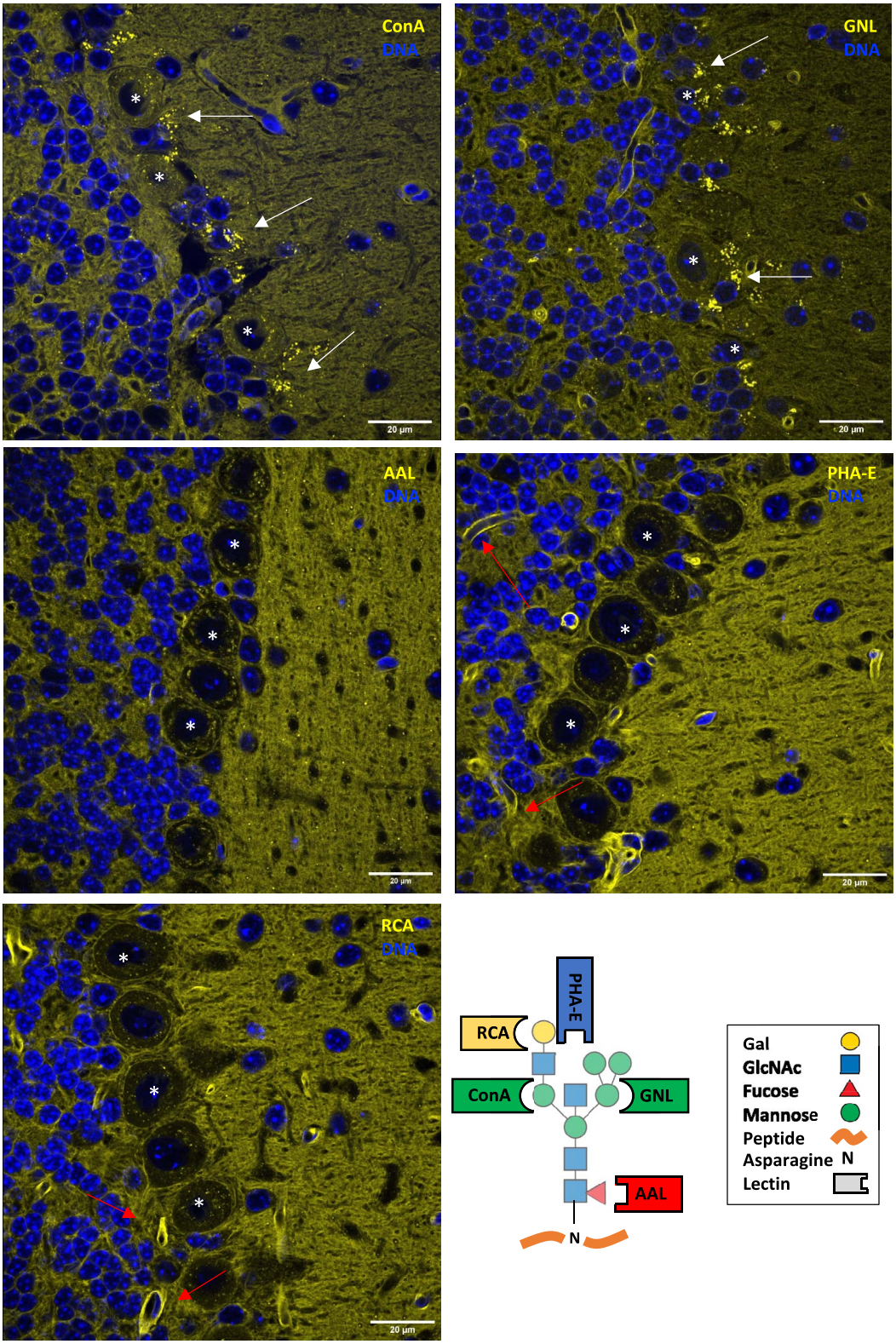

Fig. 2. N-glycan binding lectins highlight distinct structural elements at the Purkinje cell junction of the cerebellum. In addition to diffuse binding across layers of the cerebellum, the lectins GNL and ConA showed bright punctate staining (arrows) around Purkinje cell bodies (*). Binding of AAL and PHA-E showed increased signal in the molecular layer with a few diffuse punctate structures noted. PHA-E and RCA showed bright signal in multiple luminal structures consistent with microvasculature (arrows). Scale bar = 20 μm. A schematic with common lectin-binding sites is shown for reference. Individual panels are presented in supplemental material with additional context for each lectin.

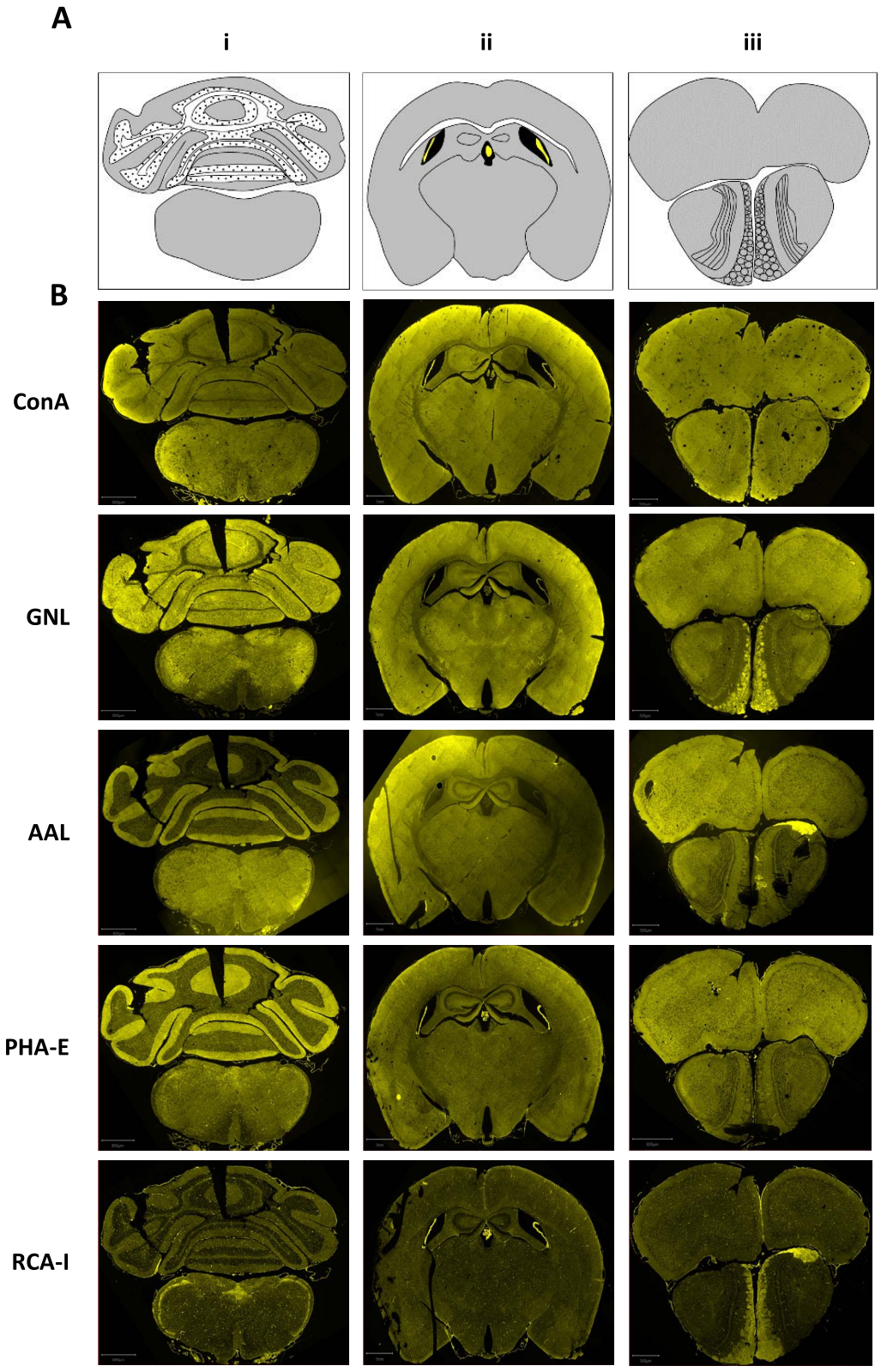

Fig. 3. N-glycan binding lectins display distinctive patterns across the brain. A) Schematic of the different coronal brain sections, highlighting prominent structures including gray matter, white matter, ventricles, and choroid. B) Staining of the different brain sections with the indicated lectins. Scale bars: i = 800 μm; ii = 1 mm, iii = 500 μm. Individual panels are presented in supplemental material with additional context for each lectin.

Table 1. N-glycan binding lectin properties in the brain. Abbreviations: PNGase F—Peptide:N-glycosidase F; ML—molecular layer; GL—granular layer; AV—arbor vitae; WMT—white matter tracks.

Lectin	PNGase F sensitivity	Competing sugar (200 mM)	Regional Binding Pattern*			Other notable structures
			i	ii	iii	
ConA	+	Mannose, Glucose	Diffuse in ML/GL, less in AV	Diffuse, less in WMT	Diffuse	Bright punctate structures, including around Purkinje cell body
GNL	+	Mannose, Glucose	Diffuse in ML/GL, less in AV	Diffuse, less in WMT	Diffuse with increased signal in glomerular layer	Bright punctate structures, including around Purkinje cell body
AAL	+	L-Fucose	Increased in ML, scattered in GL, decreased in AV	Diffuse, less in WMT	Diffuse	–
PHA-E	+	GalNAc, Lactose	Increased in ML, scattered in GL, decreased in AV	Diffuse	Diffuse	Bright signal in choroid plexus and moderate signal in microvasculature
RCA-I	+	Lactose, Galactose	Speckled throughout	Speckled throughout	Speckled with moderate signal in glomerular layer	Bright signal in choroid plexus and microvasculature
SNA	Partial	Lactose	Specific binding in ML and AV, non-specific in GL	Diffuse	Diffuse	Bright signal in choroid plexus
MAL-I	+	Lactose	Increased in ML, scattered in GL, decreased in AV	Diffuse, increased signal near surface	Diffuse, increased signal near surface	–

*Binding pattern in coronal sections according to Supplementary Fig. 1.

minimal residual PHA-E binding after GalNAc and lactose may be related to this combination of sugars not being the optimal inhibitor, even though the signal is originating from N-glycans. Intense binding was observed in the ML, with far less signal in both the GL and AV. Upon higher magnification in the cerebellum, several luminal structures were present suggesting some microvasculature was labeled by PHA-E, though this was not the bulk of the signal.

RCA, which has affinity to terminal β-linked galactose of N-glycans, showed a distinctive speckled pattern compared to the other lectins (Supplementary Fig. 6). In addition, there was some signal in the glomerular layer of the olfactory bulb. Specificity of the signal was confirmed by PNGase F treatment and inhibition with 200 mM lactose and 200 mM galactose. The speckled pattern, which was present across each region and contributed to most of the signal, was prominent in the cerebellum as luminal structures consistent with microvasculature. Minor signal was noted in the AV and ML with the least observed in the GL.

SNA, which is commonly used as a marker for glycans containing α-2,6 linked sialic acid (Bojar et al. 2022), but can also bind sulfated N-glycans, showed relatively broad binding (Supplementary Fig. 7). However, the specificity of the signal was not uniform, as PNGase F treatment and inhibition with 200 mM lactose failed to remove all binding. Strong SNA signal remained in the GL, while that in the ML and AV was reduced.

MAL-I, which binds α-2,3 sialic acid and 3-O-sulfated glycans (Geisler and Jarvis 2011), exhibited a unique binding profile unique from the other lectins tested (Supplementary Fig. 8). Binding specificity was confirmed with PNGase F and 200 mM lactose inhibition, with the latter condition leaving trace staining within Purkinje cell bodies. The most intense MAL-I binding was observed in the ML, with far less signal seen in other layers of the cerebellum and brain stem. On high magnification, several luminal structures were noted suggestive of some staining to the microvasculature.

Discussion and conclusion

In prior studies of the brain protein N-glycome, measured with both MALDI-TOF MS and lectin blotting, we observed an abundance of high mannose, bisected, and fucosylated N-glycan structures, with a scarcity of galactosylated and sialylated species (Williams et al. 2022). Here, we extended these findings to address the distribution of major N-glycan classes using optimized lectin fluorescence across the mammalian brain. The patterns suggest a level of a spatial regulation related to their functions, with the bulk of N-glycans showing diffuse distribution and more complex and modified structures showing a more restricted pattern.

ConA binds most N-glycans and GNL binds the high mannose structures that comprise the bulk of brain N-glycans (~60%); thus, their similar patterns are consistent with prior studies (Williams et al. 2022). The identity of the ConA+ and GNL+ puncta surrounding Purkinje Cell bodies are unknown but suggest that high mannose structures are enriched in specific subcellular structures, which could represent organelles including the ER/Golgi or potentially synapses. Using cultured neurons, Hanus et al. observed surface puncta of ConA that colocalized with bassoon, suggesting these glycans are enriched in synapses (Hanus et al.

2016). Govind and colleagues have also observed changes in lectin binding at synapses upon activation, suggesting different glycan structures play a dynamic role in cultured neurons (Govind et al. 2021).

AAL and PHA-E, which respectively show affinity to the fucosylated and bisected structures that make up the next major independent category of brain N-glycans (~30%), also displayed a complementary pattern of binding, supporting our previous findings of their shared presence on the same N-glycans (Williams et al. 2022). AAL and PHA-E also exhibited enrichment in the synapse rich molecular layer of the cerebellum. These results are consistent with two recent studies using LC-MS of synaptic N-glycans from rodents. Matties et al. reported high mannose glycans as the most abundant glycan in these structures, followed by fucosylated and bisected structures (Matthies et al. 2021). Bradberry et al. also found an abundance of high mannose N-glycans in synaptosomes, which a particular enrichment of fucosylated N-glycans linked to synaptic vesicle glycoproteins (Bradberry et al. 2023).

Localization of less abundant N-glycan classes, such as those containing galactose and sialic acid, present additional challenges for study. The strongest RCA signal was within microvasculature structures of the brain, in contrast with the other N-glycan binding lectins which displayed high signals in the parenchyma itself. However, this result may be complicated by the presence of the abundant α-1,3 linked fucose to the galactose-GlcNAc-fucose containing Lewis X motif in brain, and also perhaps by sulfation of galactose, which likely impairs RCA binding based on data from the NCFG glycan array. RCA binding was enriched in some unique areas, such as the area postrema, a brain stem area of increased permeability, and ventricular choroid structures. The binding of SNA and MAL-I to sialic acid-containing glycans is challenging to interpret due to several factors beyond the fact that these N-glycans are of even low abundance in the brain. These lectins can have affinity to other structures such as sulfated glycans and negatively charged galactose, without directly recognizing the sialic acid itself, and lactose is the recommended inhibiting sugar for both SNA and MAL-I, highlighting the complexity of interpreting their binding and the use of proper controls. However, both SNA and MAL-I showed affinity to ventricular choroid structures, and the striking binding of MAL-I almost exclusively to the molecular layer of the cerebellum is of particular interest and will warrant future studies. Minami et al., suggest that dynamic regulation of sialic acid is involved in memory processing, and show a decrease of MAL-I binding following acute hippocampal slice depolarization, though lectin controls were not presented (Minami et al. 2017).

In summary, we present an N-glycan landscape across the murine brain, showing distinct structural and spatial distribution of N-glycan classes. These findings complement our studies and those of others using mass spectrometry and lectin blotting to explore the unique characteristics of protein glycosylation in the mammalian brain (Lee et al. 2020; Williams et al. 2022), adding a validated and simple approach to explore glycan location. MALDI imaging is a promising and emerging tool for glycan visualization in fixed tissue that combines glycan release with mass spectrometry, generating a dataset with molecular resolution down to individual glycan masses (Hasan et al. 2021). However, the spatial resolution of MALDI imaging is currently limited at best to the micrometer range, which prevents its application to specialized structures such as dendritic spines. A full understanding of N-glycosylation in the brain will require a combination of techniques and models, each adding an essential piece to this complex puzzle.

Acknowledgments

We acknowledge the Protein-Glycan Interaction Resource of the CFG and the National Center for Functional Glycomics (NCFG) at Beth Israel Deaconess Medical Center, Harvard Medical School (https://research.bidmc.org/ncfg) (supporting grant R24GM137763). We would like to thank the Beth Israel Deaconess Medical Center Microscopy Core for technical support.

Author contributions

Maxence Noel (Conceptualization [equal], Data curation [equal], Formal analysis [equal], Investigation [equal], Methodology [equal]), Richard Cummings (Conceptualization, Data curation, Formal analysis, Funding acquisition [equal], Investigation, Methodology), and Robert Mealer (Conceptualization [equal], Data curation [equal], Formal analysis [equal], Investigation [equal], Methodology [equal])

Supplementary material

Supplementary material is available at *Glycobiology Journal* online.

Funding

This work was supported by the National Institutes of Health [R24GM137763 to R.D.C., and K08MH128712 to R.G.M.]; and The Brain & Behavior Research Foundation [30505 to R.G.M.].

Conflict of interest statement: None declared.

Data availability

The data underlying this article are available in the article and in its online supplementary material.

References

Baenziger JU, Fiete D. Structural determinants of concanavalin a specificity for oligosaccharides. *J Biol Chem*. 1979:**254**(7):2400–2407.

Bojar D, Meche L, Meng G, Eng W, Smith DF, Cummings RD, Mahal LK. A useful guide to lectin binding: machine-learning directed annotation of 57 unique lectin specificities. *ACS Chem Biol*. 2022:**17**(11):2993–3012.

Bradberry MM, Peters-Clarke TM, Shishkova E, Chapman ER, Coon JJ. N-glycoproteomics of brain synapses and synaptic vesicles. *Cell Rep*. 2023:**42**(4):112368.

Cummings RD, Kornfeld S. Characterization of the structural determinants required for the high affinity interaction of asparagine-linked oligosaccharides with immobilized Phaseolus vulgaris leukoagglutinating and erythroagglutinating lectins. *J Biol Chem*. 1982:**257**(19):11230–11234.

Cummings RD, Darvill AG, Etzler ME, Hahn MG, Varki A, Cummings RD, Esko JD, Stanley P, Hart GW, Aebi M, et al. Glycan-recognizing probes as tools. In: Varki A, Cummings RD, Esko JD, et al., editors. *Essentials of Glycobiology*. 4th ed. Cold Spring Harbor (NY): Cold Spring Harbor Laboratory Press; 2022

Freeze HH, Eklund EA, Ng BG, Patterson MC. Neurological aspects of human glycosylation disorders. *Annu Rev Neurosci*. 2015:**38**(1):105–125.

Geisler C, Jarvis DL. Effective glycoanalysis with Maackia amurensis lectins requires a clear understanding of their binding specificities. *Glycobiology*. 2011:**21**(8):988–993.

Govind AP, Jeyifous O, Russell TA, Yi Z, Weigel AV, Ramaprasad A, Newell L, Ramos W, Valbuena FM, Casler JC, et al. Activity-dependent Golgi satellite formation in dendrites reshapes the neuronal surface glycoproteome. *elife*. 2021:**10**:e68910.

Hanus C, Geptin H, Tushev G, Garg S, Alvarez-Castelao B, Sambandan S, Kochen L, Hafner AS, Langer JD, Schuman EM. Unconventional secretory processing diversifies neuronal ion channel properties. *elife*. 2016:**5**:e20609.

Hasan MM, Mimi MA, Mamun MA, Islam A, Waliullah ASM, Nabi MM, Tamannaa Z, Kahyo T, Setou M. Mass spectrometry imaging for glycome in the brain. *Front Neuroanat*. 2021:**15**:711955.

Kaku H, Goldstein IJ. Snowdrop lectin. *Methods Enzymol*. 1989:**179**: 327–331.

Klarić TS, Lauc G. The dynamic brain N-glycome. *Glycoconj J*. 2022:**39**(3):443–471.

Kornfeld R, Ferris C. Interaction of immunoglobulin glycopeptides with concanavalin A. *J Biol Chem*. 1975:**250**(7):2614–2619.

Larsen ISB, Narimatsu Y, Joshi HJ, Siukstaite L, Harrison OJ, Brasch J, Goodman KM, Hansen L, Shapiro L, Honig B, et al. Discovery of an O-mannosylation pathway selectively serving cadherins and protocadherins. *Proc Natl Acad Sci U S A*. 2017:**114**(42):11163–11168.

Lee J, Ha S, Kim M, Kim SW, Yun J, Ozcan S, Hwang H, Ji IJ, Yin D, Webster MJ, et al. Spatial and temporal diversity of glycome expression in mammalian brain. *Proc Natl Acad Sci U S A*. 2020:**117**(46): 28743–28753.

Matthies I, Abrahams JL, Jensen P, Oliveira T, Kolarich D, Larsen MR. *N* -glycosylation in isolated rat nerve terminals. *Mol Omics*. 2021:**17**(4):517–532.

Mealer RG, Williams SE, Noel M, Yang B, D'Souza AK, Nakata T, Graham DB, Creasey EA, Cetinbas M, Sadreyev RI, et al. The schizophrenia-associated variant in SLC39A8 alters protein glycosylation in the mouse brain. *Mol Psychiatry*. 2022:**27**(3):1405–1415.

Minami A, Meguro Y, Ishibashi S, Ishii A, Shiratori M, Sai S, Horii Y, Shimizu H, Fukumoto H, Shimba S, et al. Rapid regulation of sialidase activity in response to neural activity and sialic acid removal during memory processing in rat hippocampus. *J Biol Chem*. 2017:**292**(14):5645–5654.

Rebelo AL, Contessotto P, Joyce K, Kilcoyne M, Pandit A. An optimized protocol for combined fluorescent lectin/immunohistochemistry to characterize tissue-specific glycan distribution in human or rodent tissues. *STAR Protoc*. 2021:**2**(1):100237.

Samal J, Saldova R, Rudd PM, Pandit A, O'Flaherty R. Region-specific characterization of N-glycans in the striatum and substantia Nigra of an adult rodent brain. *Anal Chem*. 2020:**92**(19): 12842–12851.

Sevillano AM, Aguilar-Calvo P, Kurt TD, Lawrence JA, Soldau K, Nam TH, Schumann T, Pizzo DP, Nyström S, Choudhury B, et al. Prion protein glycans reduce intracerebral fibril formation and spongiosis in prion disease. *J Clin Invest*. 2020:**130**(3): 1350–1362.

Shibuya N, Goldstein IJ, Broekaert WF, Nsimba-Lubaki M, Peeters B, Peumans WJ. The elderberry (Sambucus nigra L.) bark lectin recognizes the Neu5Ac(alpha 2-6)Gal/GalNAc sequence. *J Biol Chem*. 1987:**262**(4):1596–1601.

Suttapitugsakul S, Stavenhagen K, Donskaya S, Bennett DA, Mealer RG, Seyfried NT, Cummings RD. Glycoproteomics landscape of asymptomatic and symptomatic human Alzheimer's disease brain. *Mol Cell Proteomics*. 2022:**21**(12):100433.

Wang WC, Cummings RD. The immobilized leukoagglutinin from the seeds of Maackia amurensis binds with high affinity to complex-type Asn-linked oligosaccharides containing terminal sialic acid-linked alpha-2,3 to penultimate galactose residues. *J Biol Chem*. 1988:**263**(10):4576–4585.

Williams SE, Noel M, Lehoux S, Cetinbas M, Xavier RJ, Sadreyev RI, Scolnick EM, Smoller JW, Cummings RD, Mealer RG. Mammalian brain glycoproteins exhibit diminished glycan complexity compared to other tissues. *Nat Commun*. 2022:**13**(1):275.

Wright CS, Hester G. The 2.0 a structure of a cross-linked complex between snowdrop lectin and a branched mannopentaose: evidence for two unique binding modes. *Structure*. 1996:**4**(11): 1339–1352.

Yamashita K, Kochibe N, Ohkura T, Ueda I, Kobata A. Fractionation of L-fucose-containing oligosaccharides on immobilized Aleuria aurantia lectin. *J Biol Chem*. 1985:**260**(8):4688–4693.

Zou X, Yoshida M, Nagai-Okatani C, Iwaki J, Matsuda A, Tan B, Hagiwara K, Sato T, Itakura Y, Noro E, et al. A standardized method for lectin microarray-based tissue glycome mapping. *Sci Rep*. 2017:**7**(1):43560.